ISSN 0915-633X

NATIONAL INSTITUTE FOR FUSION SCIENCE

Structure of Period-2 Step-1 Accelerator Island in Area Preserving Maps

K. Hirose, S. Saitô and Yoshi.H. Ichikawa

(Received - Feb. 27, 1996)

NIFS-408 Mar. 1996

RESEARCH REPORT
NIFS Series

NAGOYA, JAPAN

Structure of Period-2 Step-1 Accelerator Island in Area Preserving Maps

[1] *K.Hirose* [2]*S.Saitô*
and
[1]*Yoshi.H.Ichikawa*

[1]*College of Engineering, Chubu University, Kasugai,487,Japan*
[2]*School of Engineering, Nagoya University, Nagoya,464-01,Japan*

Abstract

Since the multi-periodic accelerator modes manifest their contribution even in the region of small stochastic parameters, analysis of such regular motion appears to be critical to explore the stochastic properties of the Hamiltonian system. Here, structure of period-2 step-1 accelerator mode is analyzed for the systems described by the Harper map and by the standard map. The stability criterions have been analyzed in detail in comparison with numerical analyses. The period-3 squeezing around the period-2 step-1 islands is identified in the standard map.

Keywords

Harper map, Standard map, Period-2 step-1 accelerator mode

[1]e-mail b95710@isc.chubu.ac.jp
[2]e-mail satoshi@ice.nuie nagoya-u.ac.jp

1 INTRODUCTION

Many important problems in plasma physics are well described by Hamiltonians of few degrees of freedom. The powerful approaches are the method of nonlinear dynamical maps, applied to the wandering of the magnetic field lines in plasma confinement devices [1], the confinement of energetic α -particles in tokamak plasma [2] the radial transport of ions in tandem-mirror devices [3], and the stochastic heating of the plasma by external radio-frequency waves [4]. The standard map plays the canonical role in studies of these various problems.

Stochastic aspect of the few degrees of Hamiltonian system attracts extensive interest to explore interplay between the regular and the chaotic motion. Critical issues are the effect of stickiness of the islands in the nonlinear dynamical map [5]. Ichikawa et al [6], have carried out extensive numerical studies of stochastic diffusion in the standard map, observing that various multi-periodic accelerator modes even in the region of small stochastic parameter give rise to anomalous enhancement of diffusion. Recent study of the Harper map [7] has shown very clear enhancement of the stochastic diffusion, as the result of the period-2 step-1 accelerator mode.

In the present study, we have carried out analysis of structure of the period-2 step-1 accelerator islands of the Harper map [7] in the second section, and of the standard map [6] referring to the list of period-p step-1 accelerator modes of the standard map in the third section. The last section is devoted to concluding remarks.

2 THE HARPER MAP

Saitô et al [7], have studied the anomalous diffusion associated with the Harper map,

$$\begin{aligned} q_{n+1} &= q_n - \frac{L}{2\pi}\sin(2\pi p_{n+1}) \\ p_{n+1} &= p_n + \frac{A}{2\pi}\sin(2\pi q_n) \qquad \text{(mod 1)} \end{aligned} \tag{1}$$

when n stands for the discrete time step. L and A are positive stochastic parameters. Their numerical observation indicates clear evidence of the enhanced contribution of the period-2 step-1 accelerator mode at $A \approx 3.2$, and of the period-2 step-3 accelerator mode at $A \approx 9.4$.

The second iteration of the Harper map Eq.1, gives rise to

$$\begin{aligned} q_{n+2} &= q_n - \frac{L}{2\pi}\sin(2\pi p_n + A\sin(2\pi q_n)) \\ &\quad -\frac{L}{2\pi}\sin[(2\pi p_n + A\sin(2\pi q_n) \\ &\quad +A\sin\{2\pi q_n - L\sin(2\pi q_n + A\sin(2\pi q_n))\}], \qquad (2) \\ p_{n+2} &= p_n + \frac{A}{2\pi}\sin(2\pi q_n) \\ &\quad +\frac{A}{2\pi}\sin\{2\pi q_n - L\sin(2\pi p_n + A\sin(2\pi q_n))\}. \qquad (3) \end{aligned}$$

The coordinates (q_0, p_0) of the period-2 step-1 accelerator mode are determined from the condition

$$\frac{A}{2\pi}\sin(2\pi q_0) + \frac{A}{2\pi}\sin(2\pi q_0 - L\sin(2\pi p_0 + A\sin(2\pi q_0))) = 1. \qquad (4)$$

According to the observation of Saitô et al [7], however, we see that $p_0 = 0$ and hence we may determine the coordinate q_0 from the condition

$$\frac{A}{2\pi}\sin(2\pi q_0) = \frac{1}{2} \qquad (5)$$

which is consistent with Eq.(4) with $p_0 = 0$. For the period-2 step-3 accelerator mode, we have the condition

$$\frac{A}{2\pi}\sin(2\pi q_0) = \frac{3}{2}. \qquad (6)$$

It is straightforward to calculate the tangent map of the squared Harper map, which in turn gives rise to the trace of the tangent map as

$$Tr(\delta H^2) = 2 - AL[\cos(2\pi q_n) + \cos\{2\pi q_n - L\sin(2\pi p_n + A\sin 2\pi q_n)\}]$$

$$[\cos(2\pi p_n + A\sin 2\pi q_n) + \cos\{2\pi p_n + A\sin 2\pi q_n$$
$$+ A\sin\{2\pi q_n - L\sin(2\pi p_n + A\sin 2\pi q_n)\}\}]$$
$$+ (AL)^2 \cos\{2\pi p_n + A\sin 2\pi q_n + A\sin\{2\pi q_n - L\sin(2\pi p_n + A\sin 2\pi q_n)\}\}$$
$$\cos\{2\pi q_n - L\sin(2\pi p_n + A\sin 2\pi q_n)\}\cos\{2\pi p_n + A\sin 2\pi q_n\}\cos(2\pi q_n). \tag{7}$$

Referring to Eqs (5) and (6), we have the coordinate of the period-2 step-s accelerator modes as

$$q_0 = \frac{1}{2\pi}\sin^{-1}\left(\frac{s\pi}{A}\right), \qquad p_0 = 0. \tag{8}$$

where s equals to 1 or 3. Now, the Green's residue R is determined as

$$R = \frac{1}{4}(AL)^2\cos^2(2\pi q_0), \tag{9}$$

which gives rise to stability condition

$$0 < R < 1. \tag{10}$$

Thus, we can determine the stable region as

$$s\pi < A < \left((s\pi)^2 + \frac{4}{L^2}\right)^{\frac{1}{2}} \tag{11}$$

with $s = 1$ and $s = 3$ for the period-2 step-1 and the period-2 step-3 accelerator mode, respectively. For the special case of L=A, Eq.11 is reduced to

$$s\pi < A < \left(\frac{(s\pi)^2}{2} + \sqrt{4 + \frac{(s\pi)^4}{4}}\right)^{\frac{1}{2}}. \tag{12}$$

Here, we get $\pi < A < 3.203$ for $s = 1$, and $3\pi < A < 9.427$ for $s = 3$, respectively.

Let us illustrate firstly period doubling bifurcation of the stable period-2 step-1 accelerator modes for a value of $L = 3.3$ in Fig.1.a) and Fig.1.b). According to

Eq.(11), we get the critical value of $A = 3.1995$. Fig.1.a) shows the island structures at $p_0 = 0, q_0 = 0.2803$ which undergoes the period doubling bifurcation for $A = 3.2$ and $L = 3.3$ as shown in Fig.1.b)

For the special case of A=L , according to Eq.(12), the stable island at $A = L = 3.203$ shown in Fig.2.a) undergoes the period doubling bifurcation at the value of $A = L = 3.204$ as shown in Fig.2.b)

It is interesting to note that in these figures the other island at $p_0 = 0, q_0 = 0.2197$ are strongly elongated into the direction of momentum p.

We conclude the present section by noting that for the case of small limit of the stochastic parameter L, there appears the invariant surface $q = const$, while the period-2 step-1 accelerator mode persist to exist. Fig.3.a) and Fig.3.b) illustrate the phase portrait of the Harper map for the values of $A = 3.18$, $L = 1.0$ and of $A = 3.18, L = 0.1$, respectively. In Fig.3.b), we observe the period-3 step-1 accelerator mode as well besides the pair of the period-2 step-1 accelerator mode. Their transition between the regular and the stochastic motion in the p-direction for the given value of A, will be discussed in our future study.

3 THE STANDARD MAP

Turning to our interest to the standard map,

$$\begin{aligned} q_{n+1} &= q_n + p_{n+1} \\ p_{n+1} &= p_n + A\sin(2\pi q_n) \qquad \pmod 1. \end{aligned} \tag{13}$$

Ichikawa et al [6], have observed of period-4 step-2 accelerator mode in the region of $0.6420 < A < 0.6540$. Anticipating that this might be a period-2 step-1 mode, we have carried out careful numerical observation. The phase space diagram Fig.4 of the standard map at $A = 0.6425$ indicates coherent structures at $(p_0 \approx 0.2, q_0 \approx 0.3)$ and $(p_0 \approx -0.2, q_0 \approx 0.1)$, confirming the previous observation that these modes are pronounced at $p_0 \approx 0.2$. We have succeeded to extract the orbit, showing the period-2 step-1 acceleration as illustrated in Fig.5.a), while Fig.5.b) shows that the orbit started at $p_0 = -0.205, q_0 = 0.106$ detraps from the period-2 step-1 orbit after the 58 time steps, and then subjects to stochastic wandering.

Now, we will analyze structures of the period-2 step-1 accelerator islands. Since the second iterated standard map is written as

$$\begin{aligned} q_{n+2} &= q_n + p_n + A\sin(2\pi q_n) + p_{n+2} \\ p_{n+2} &= p_n + A\sin(2\pi q_n) + A\sin\{2\pi(q_n + p_n + A\sin(2\pi q_n))\} \end{aligned} \quad (14)$$

we can write the expression for coordinate (p_0, q_0) for the period-2 step-1 accelerator mode as

$$2p_0 + A\sin(2\pi q_0) = 0, \quad (15)$$

$$A\sin(2\pi q_0) + A\sin\{2\pi(q_0 + p_0 + A\sin(2\pi q_0))\} = 1. \quad (16)$$

Eq.(15) gives

$$p_0 = -\frac{A}{2}\sin(2\pi q_0). \quad (17)$$

Eliminating q_0 from Eq.(16) in terms of Eq.(17), we obtain

$$F(p_0) = G(A, p_0) \quad (18)$$

with the abbreviations of

$$F(p) = 1 + 2p + 2p\cos(2\pi p) \quad (19)$$

and

$$G(A, p) = -\sqrt{A^2 - 4p^2}\sin(2\pi p). \quad (20)$$

Eq.(18) determines the momentum $p_0(A)$ for a given value of A, which in turn determines the coordinate q_0 as

$$q_0 = \frac{1}{2\pi}\sin^{-1}\left(-\frac{2p_0}{A}\right). \quad (21)$$

Solving numerically Eq.(18) in the region of $0.641 < A < 0.650$, we obtain the following set of solutions as listed in Table 1.

A	p	q
0.641	$p_1 = -0.1904$	$q_1 = 0.1016$
	$p_2 = -0.1999$	$q_2 = 0.1066$
0.642	$p_1 = -0.1876$	$q_1 = 0.0995$
	$p_2 = -0.2029$	$q_2 = 0.1089$
0.6425	$p_1 = -0.1856$	$q_1 = 0.0982$
	$p_2 = -0.2050$	$q_2 = 0.1100$
0.644	$p_1 = -0.1840$	$q_1 = 0.0968$
	$p_2 = -0.2068$	$q_2 = 0.1111$
0.646	$p_1 = -0.1814$	$q_1 = 0.0095$
	$p_2 = -0.2098$	$q_2 = 0.1127$
0.6465	$p_1 = -0.1808$	$q_1 = 0.0946$
	$p_2 = -0.2105$	$q_2 = 0.1132$
0.650	$p_1 = -0.1774$	$q_1 = 0.0914$
	$p_2 = -0.2146$	$q_2 = 0.1149$

Now, we proceed to analyze the stability of these two sets of the period-2 step-1 accelerator mode. The residue of the tangent map of the Eq.(14), is calculated straightforwardly as

$$R = 1 - \{1 + \pi A\cos(2\pi q_n)\}\{1 + \pi A\cos(2\pi(q_n + p_n + A\sin(2\pi q_n)))\}. \tag{22}$$

The stability condition is expressed as

$$0 < \{1 + \pi A\cos(2\pi q_0)\}\{1 + \pi A\cos 2\pi(q_0 - p_0)\} < 1. \tag{23}$$

Substituting the above values of (q_1, p_1) and (q_2, p_2) for the given value of A into Eq.(23), we find that the set of (q_2, p_2) is stable up to $A = 0.651$ which turns into unstable at $A = 0.6513$ with $(q_2, p_2) = (0.11536, 0.21591)$.

The onset condition of the period-2 step-1 accelerator mode is given as

$$\frac{d}{dp}F(p) = \frac{d}{dp}G(A, p) \tag{24}$$

together with Eq.(18). By eliminating the parameter A from Eq.(18) and Eq.(24), the momentum value p_c at which the period-2 step-1 accelerator mode appears is given as the solution of

$$\begin{aligned} 1 &+ \{1 - \pi\frac{1 + 2p(1 + \cos(2\pi p))}{\sin(2\pi p)}\} \cos(2\pi p) \\ &= 2\{\pi - \frac{\sin(2\pi p)}{1 + 2p(1 + \cos(2\pi p)}\} p \sin(2\pi p). \end{aligned} \tag{25}$$

Numerical solution of Eq.(25) gives the value of

$$p_c = -0.19512. \tag{26}$$

In terms of Eq.(18), the parameter A_c is expressed as the function of p_c,

$$A_c^2 = 4p_c^2 + \frac{1}{\sin^2 2\pi p_c}\{1 + 2p_c(1 + \cos(2\pi p_c)\}^2 \tag{27}$$

which gives rise to

$$A_c = 0.64037. \tag{28}$$

Substituting Eqs.(26) and (28) into Eq.(21), we obtain the coordinate q_c as

$$q_c = 0.1043. \tag{29}$$

Thus, we can conclude that the period-2 step-1 accelerator mode of the standard map is stable in the region of

$$0.64037 < A < 0.65130. \tag{30}$$

In the region of Eq.(30), the structure of the period-2 step-1 accelerator island undergoes very intricated changes as illustrated in Fig.6.a) and Fig.6.b). Increasing the stochastic parameter A from $A = 0.6462$ to $A = 0.6467$, we observe that the period-3 squeezing takes place around the period-2 step-1 islands as ilastrated Fig.7.a), Fig.7.b) and Fig.7.c).

4 CONCLUDING REMARK

Here, we have presented detailed analysis of structure of the period-2 step-1 accelerator mode in the area preserving maps such as the Harper map and the standard map. The analysis for the Harper map is rather simple owing to the fact that the momentum p_0 is 0. As for the standard map, the present analysis is the first attempt to analyze structure of the multi-periodic accelerator modes which contribute to the anomalous diffusion in the region of $A < 1$. We may undertake the examination of the period-3 step-1 and period-3 step-2 accelerator modes, listed in Table 1 of the reference 6.

Since the integrable accelerator orbits are densely distributed in the domain of small stochastic parameter, we anticipate that analysis of the multi periodic accelerator modes explores fundamental structure of the stochastic layer between the integrable regular motion and the nonintegrable chaotic motion. Such analysis will provides us a tool to quantify the stickiness of the stochastic layer and the long time behavior of the system. At least, we can assure that the stoachastic layer of the regular motion and chaotic motion has far more complicated structure than the simple picture portrayed by Meiss et al [5], for the transport phenomena in Hamiltonian systems.

ACKNOWLEDGEMENTS

We dedicate this paper for the memory of Vladmir Petviashvili. One of the present authors (Y.H.I) has enjoyed our friendship over the past twenty years. Professor Petviashvili was a representative of *intelligentzia* with full of inspiring spirit not only in physics, but for wide range of human activity. We pray for the repose of soul of Vladimir Petviashvili. The authors wish to express their thanks to Professor T.Kamimura for his valuable discussion. They also thank the staff of the Computer Center at the National Institute for Fusion Science (NIFS). This work was supported by the Collaborating Program of NIFS.

References

[1] J.D.Hanson, and J.R.Cary,*Phy. Fluids* **27,767**(1984)

[2] R.J.Goldstone, R.B.White, and A.H.Boozer,*Phys.Rev. Lett.* **47, 647**(1981)

[3] Y.H.Ichikawa, T.Kamimura, and C.F.F.Karney,*Physica* , **6D 233**(1983)

[4] C.F.F.Karney,*Phys. Fluids* **22, 2188**(1979)

[5] J.D.Meiss, R.S.MacKay, and I.C.Percival,*Physica* **13D,55**(1984)

[6] Y.H.Ichikawa, T.Kamimura, and T,Hatori,*Physica* **29D,247**(1987)

[7] S.Saitô, Y.Nomura, and Y.H.Ichikawa,*Prog. Theoret. Phys.* **94,745**(1995)

Captions of Figures and Table

Fig.1

a) Structure of the period-2 step-1 island at $q_0 = 0.2803$, $p_0 = 0$ for $A = 3.1995$ and $L = 3.3$, b) the period doubling bifurcation of the period-2 step-1 island at the value of $A = 3.2$ and $L = 3.3$.

Fig.2

a) Structure of the period-2 step-1 island for $A = L = 3.203$,b) the period doubling bifurcation at the value of $A = L = 3.204$.

Fig.3

Phase space portrait of the Harper map, a) for values of $A = 3.185$ and $L = 1.0$, and b) for values of $A = 3.185$ and $L = 0.1$.

Fig.4

Phase space portrait of the standard map for $A = 0.6425$. The orbits are started at the initial points distributed uniformly in the region of $0.105 < q_0 < 0.110$ at $p_0 = -0.184$.

Fig.5

The temporal evolution of the orbits, a) started at $q_0 = 0.106$, $p_0 = -0.200$ and b) started at $q_0 = 0.106$, $p_0 = -0.205$ for $A = 0.6425$.

Fig.6

Island structure of the period-2 step-1 accelerator mode a) for $A = 0.6425$, and b) for $A = 0.6460$.

Fig.7

Period-3 squeezing arround the period-2 step-1 accelerator mode in the process of increasing A, a) $A = 0.6462$, b) $A = 0.64635$ and c) $A = 0.6467$.

Table 1

Position of the period-2 step-1 accelerator modes. The sets of (p_1, q_1) are unstable for the stochastic parameter $A > 0$. The sets of (p_2, q_2) are stable for the range of $0.64037 < A < 0.65130$.

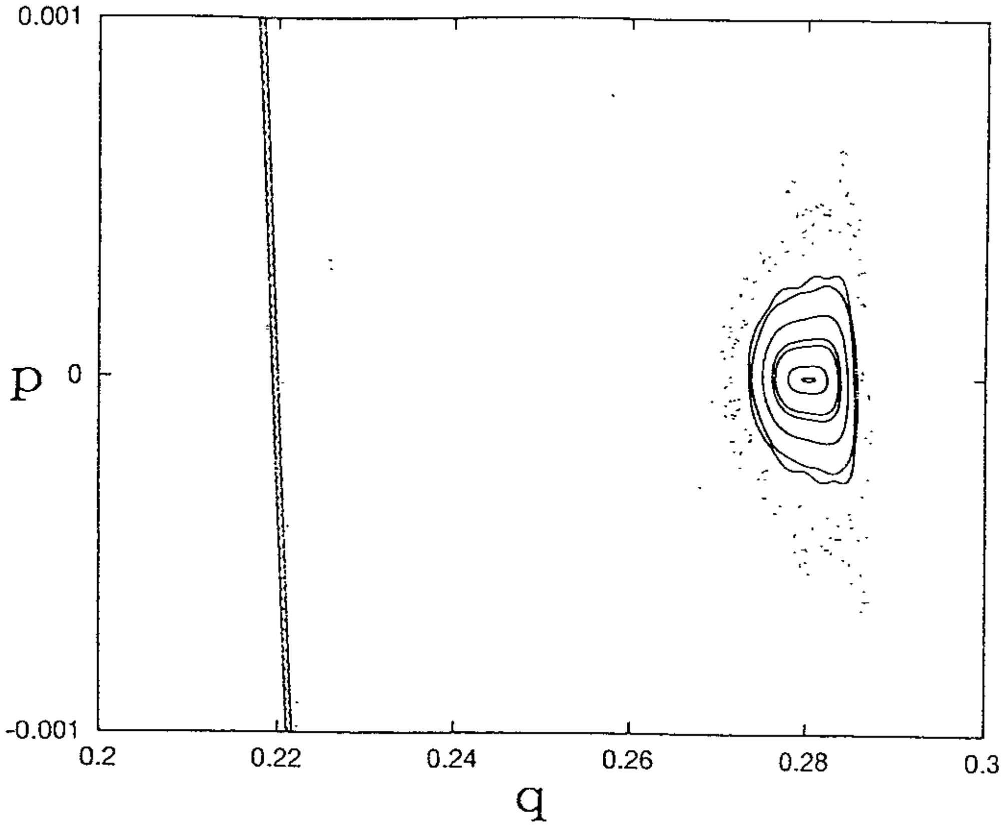
0.001
p 0
-0.001
0.2
0.22
0.24
0.26
0.28
0.3
q

Fig 1a)

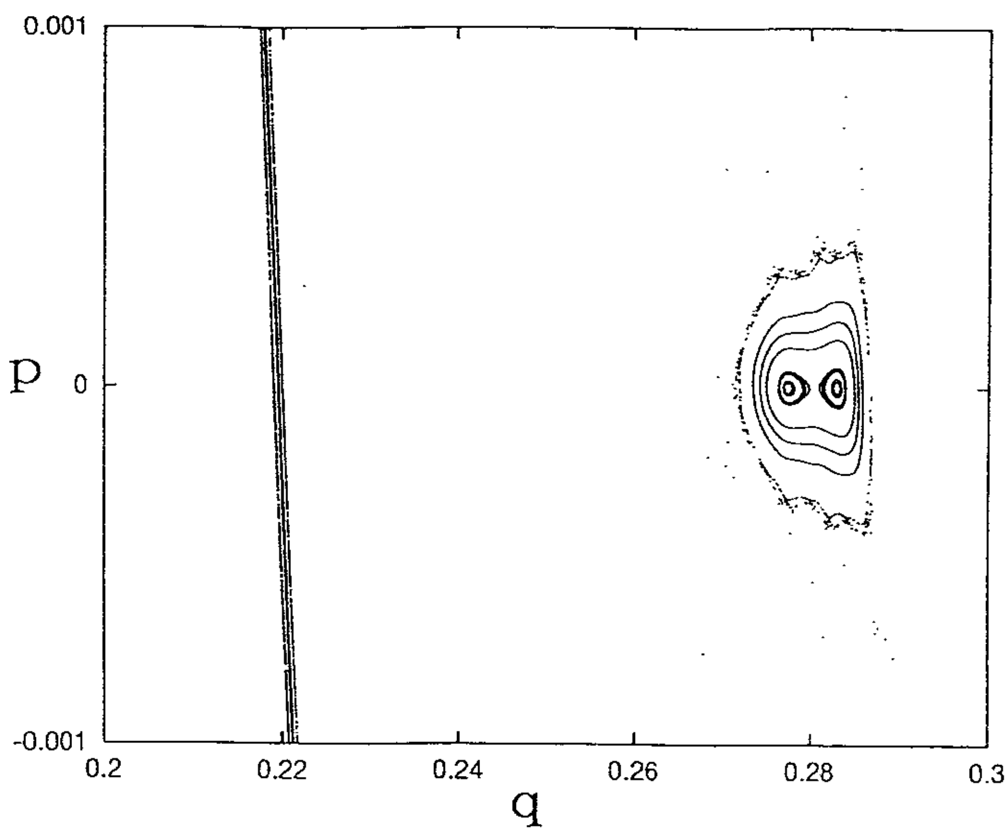
0.001
p 0
-0.001
0.2
0.22
0.24
0.26
0.28
0.3
q

Fig 1b)

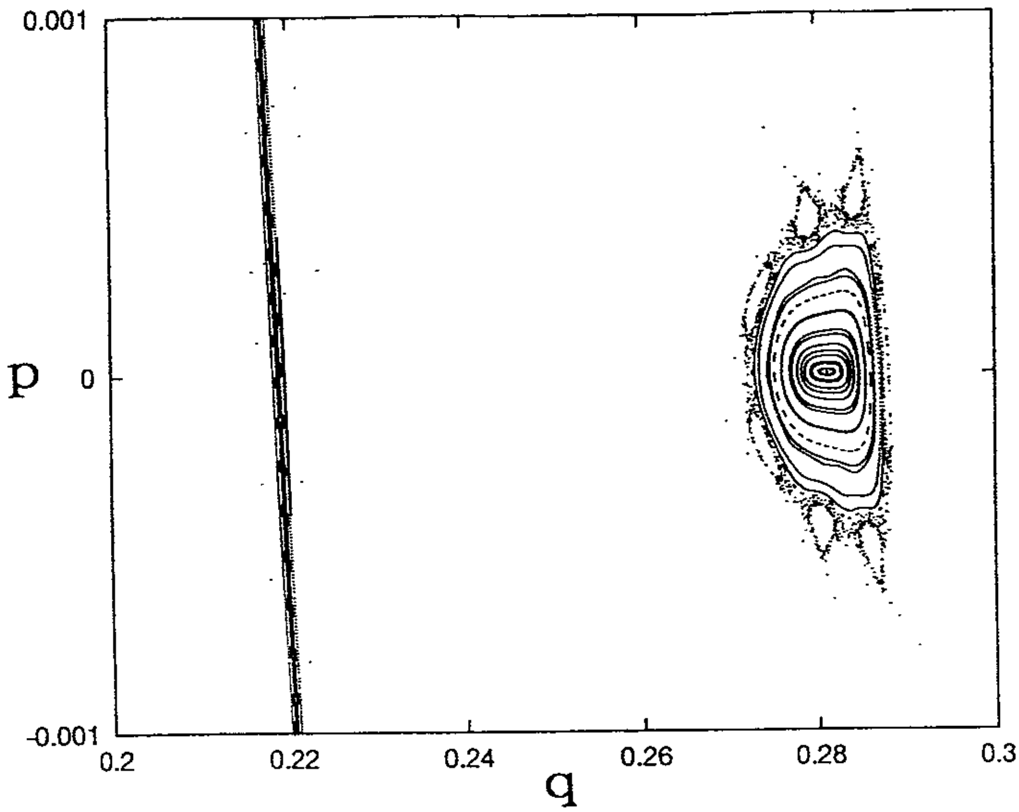
0.001
p
0
-0.001
0.2
0.22
0.24
0.26
0.28
0.3
q

Fig 2a)

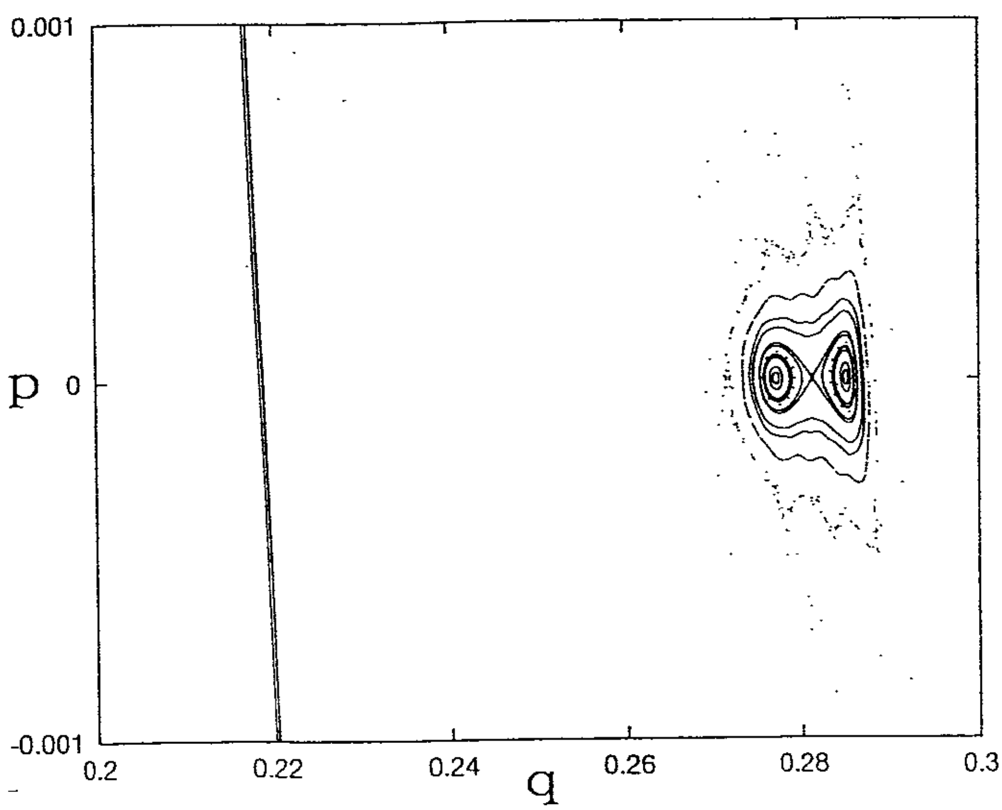
0.001
p
0
-0.001
0.2
0.22
0.24
0.26
0.28
0.3
q

Fig 2b)

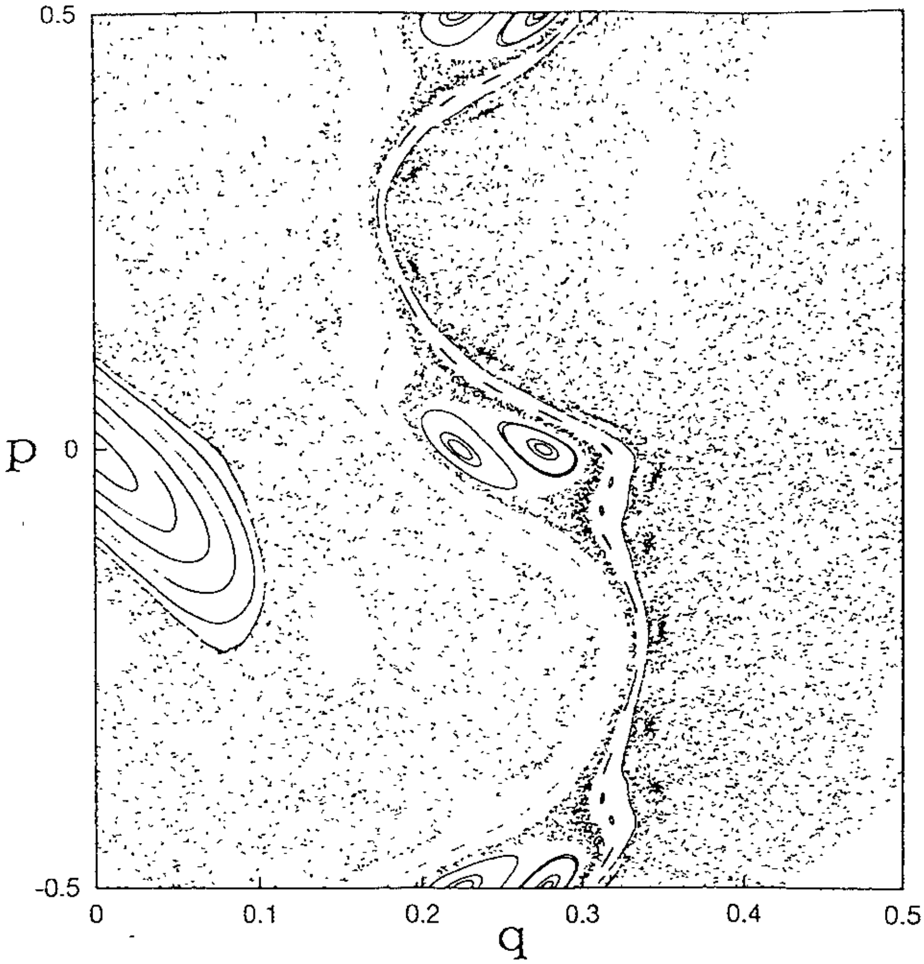

Fig 3a)

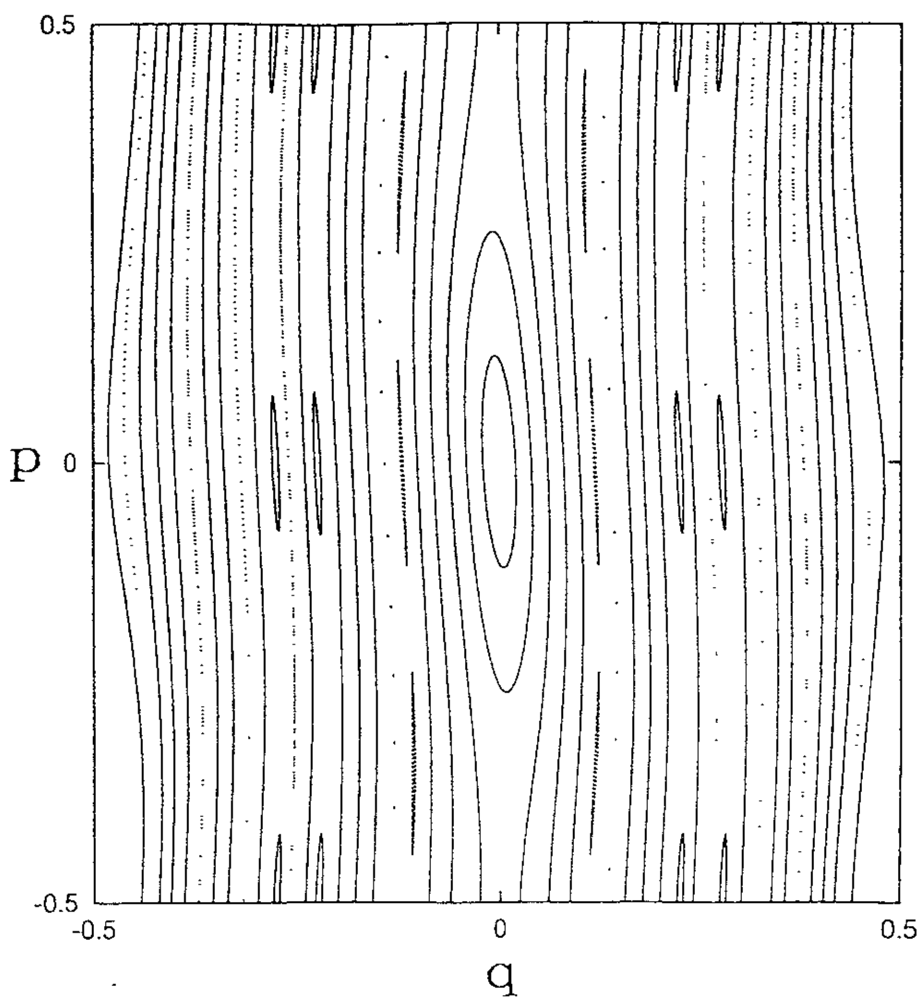

Fig 3b)

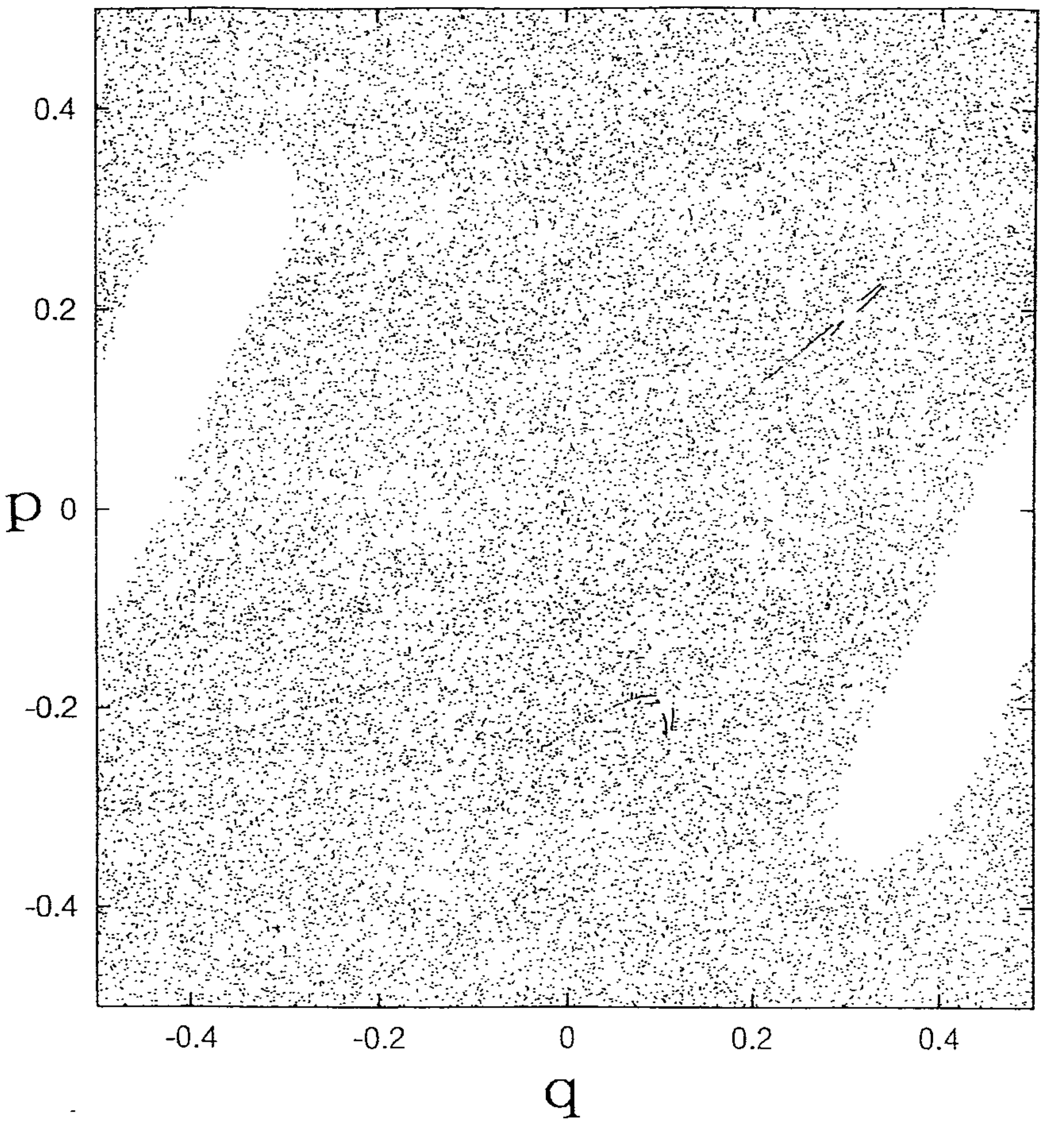

Fig 4

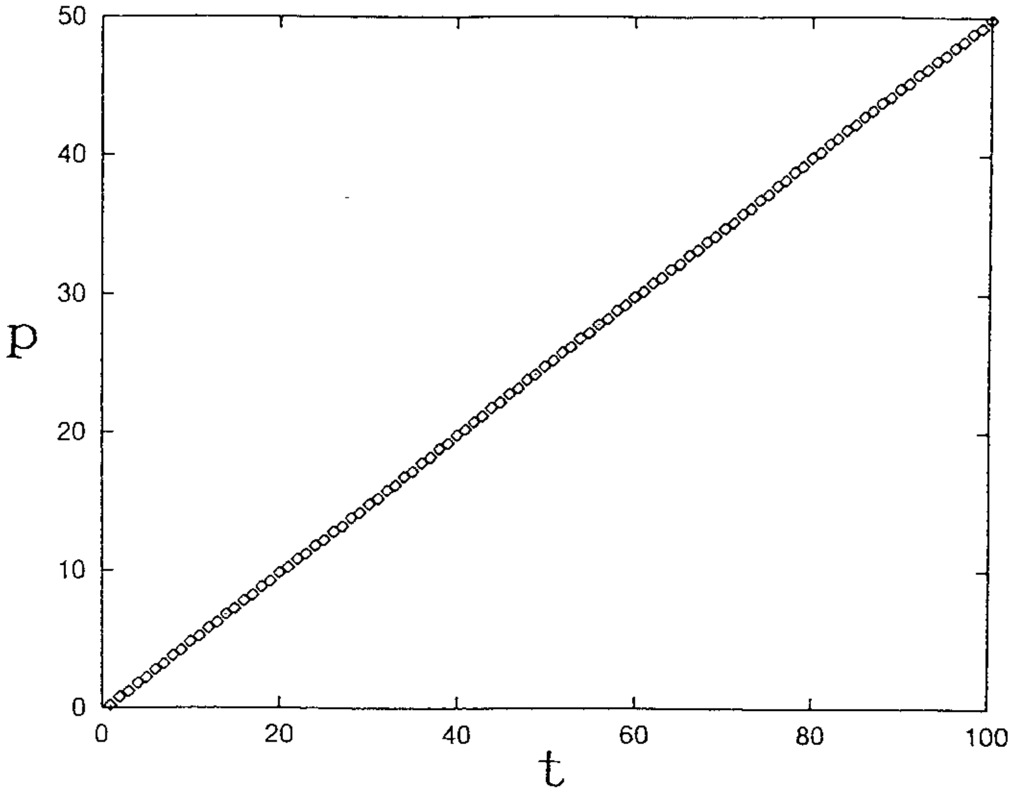
50
40
30
20
10
0
p
0
20
40
60
80
100
t

Fig 5a)

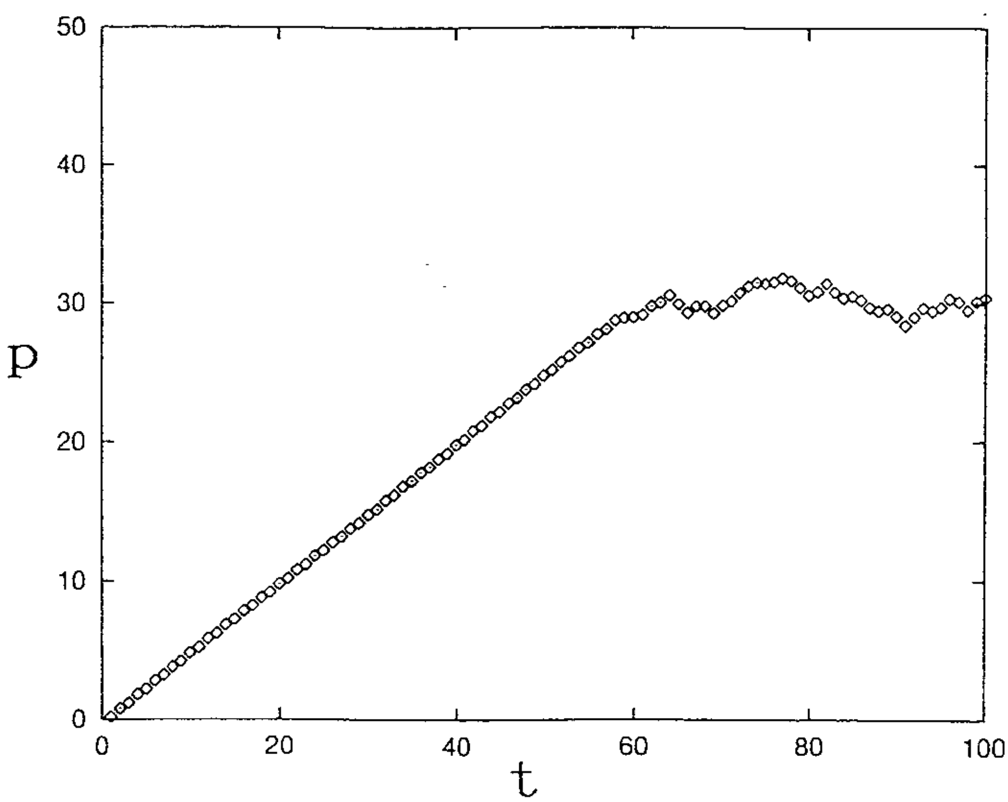
50
40
30
20
10
0
p
0
20
40
60
80
100
t

Fig 5b)

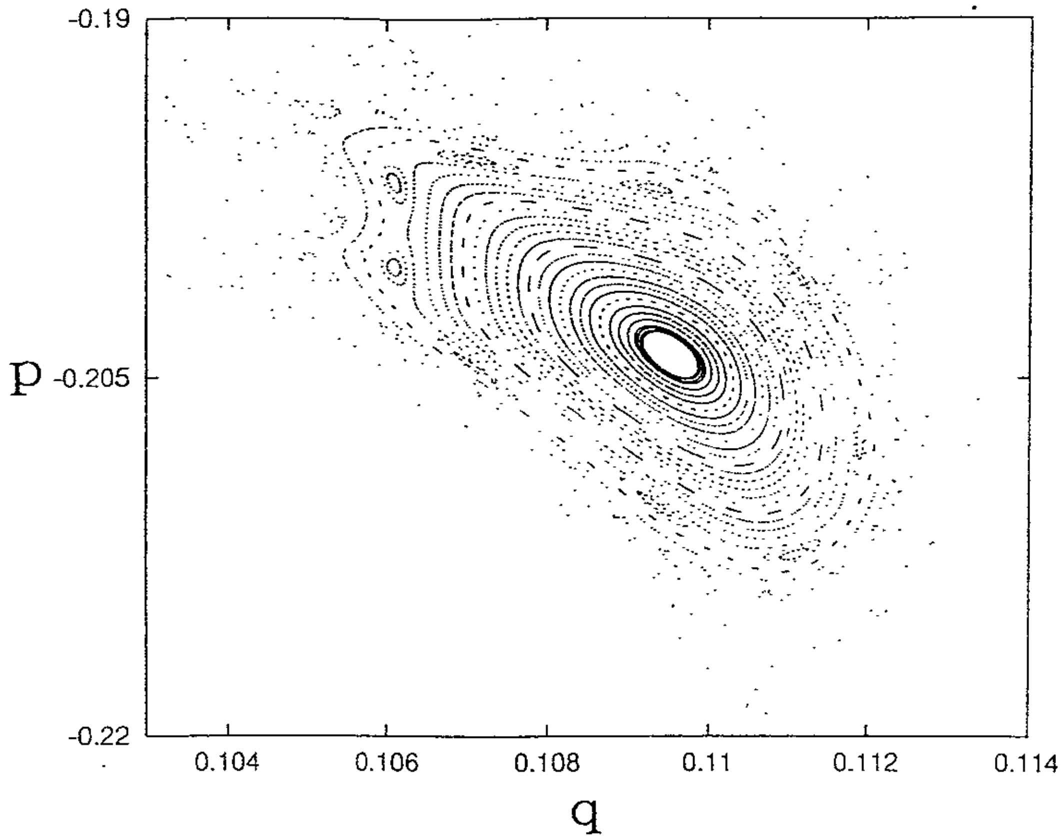

-0.19
p -0.205
-0.22
0.104
0.106
0.108
0.11
0.112
0.114
q

Fig 6a)

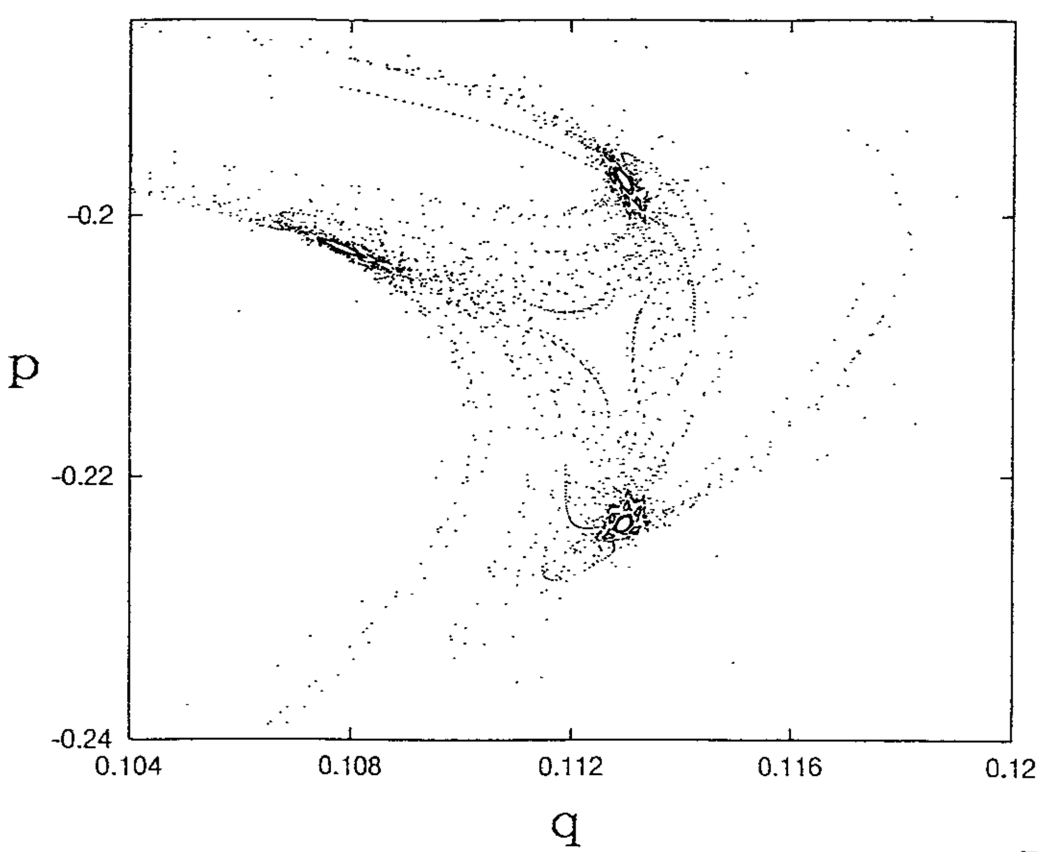

-0.2
p
-0.22
-0.24
0.104
0.108
0.112
0.116
0.12
q

Fig 6b)

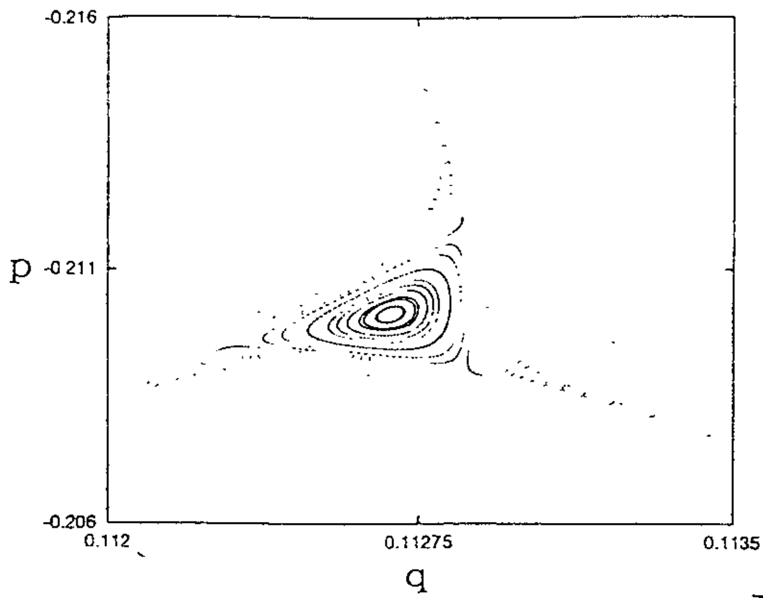

Fig 7a)

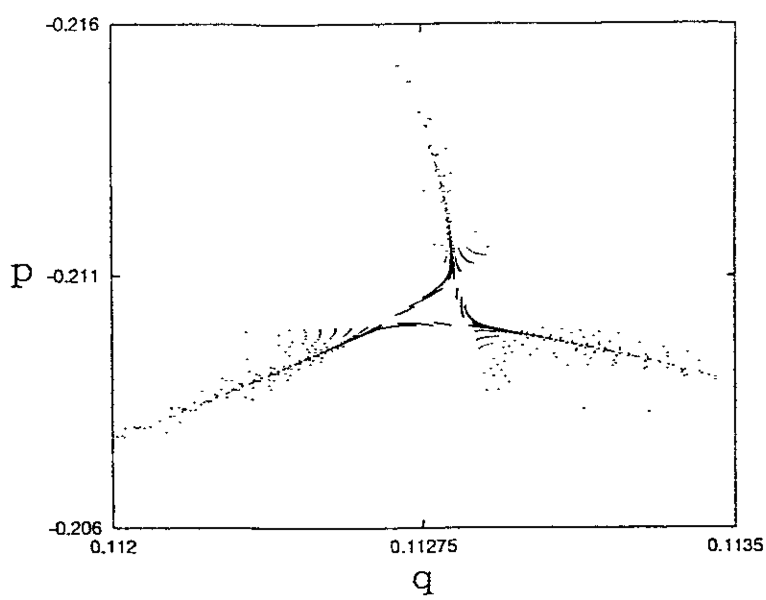

Fig 7b)

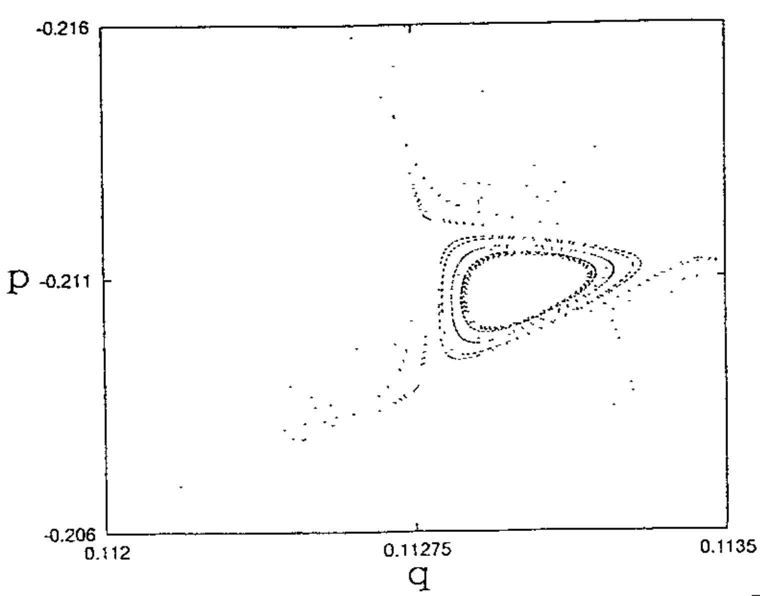

Fig 7c)

Recent Issues of NIFS Series

NIFS-361 K. Kamada, H. Kinoshita and H. Takahashi,
Anomalous Heat Evolution of Deuteron Implanted Al on Electron Bombardment; June 1995

NIFS-362 V.D. Pustovitov,
Suppression of Pfirsch-schlüter Current by Vertical Magnetic Field in Stellarators; June 1995

NIFS-363 A. Ida, H. Sanuki and J. Todoroki
An Extended K-dV Equation for Nonlinear Magnetosonic Wave in a Multi-Ion Plasma; June 1995

NIFS-364 H. Sugama and W. Horton
Entropy Production and Onsager Symmetry in Neoclassical Transport Processes of Toroidal Plasmas; July 1995

NIFS-365 K. Itoh, S.-I. Itoh, A. Fukuyama and M. Yagi,
On the Minimum Circulating Power of Steady State Tokamaks; July 1995

NIFS-366 K. Itoh and Sanae-I. Itoh,
The Role of Electric Field in Confinement; July 1995

NIFS-367 F. Xiao and T. Yabe,
A Rational Function Based Scheme for Solving Advection Equation; July 1995

NIFS-368 Y. Takeiri, O. Kaneko, Y. Oka, K. Tsumori, E. Asano, R. Akiyama, T. Kawamoto and T. Kuroda,
Multi-Beamlet Focusing of Intense Negative Ion Beams by Aperture Displacement Technique; Aug. 1995

NIFS-369 A. Ando, Y. Takeiri, O. Kaneko, Y. Oka, K. Tsumori, E. Asano, T. Kawamoto, R. Akiyama and T. Kuroda,
Experiments of an Intense H- Ion Beam Acceleration; Aug. 1995

NIFS-370 M. Sasao, A. Taniike, I. Nomura, M. Wada, H. Yamaoka and M. Sato,
Development of Diagnostic Beams for Alpha Particle Measurement on ITER; Aug. 1995

NIFS-371 S. Yamaguchi, J. Yamamoto and O. Motojima;
A New Cable -in conduit Conductor Magnet with Insulated Strands; Sep. 1995

NIFS-372 H. Miura,
Enstrophy Generation in a Shock-Dominated Turbulence; Sep. 1995

NIFS-373 M. Natsir, A. Sagara, K. Tsuzuki, B. Tsuchiya, Y. Hasegawa, O. Motojima,
Control of Discharge Conditions to Reduce Hydrogen Content in Low Z Films Produced with DC Glow; Sep. 1995

NIFS-374 K. Tsuzuki, M. Natsir, N. Inoue, A. Sagara, N. Noda, O. Motojima, T. Mochizuki, I. Fujita, T. Hino and T. Yamashina,
Behavior of Hydrogen Atoms in Boron Films during H_2 and He Glow Discharge and Thermal Desorption; Sep. 1995

NIFS-375 U. Stroth, M. Murakami, R.A. Dory, H. Yamada, S. Okamura, F. Sano and T. Obiki,
Energy Confinement Scaling from the International Stellarator Database; Sep. 1995

NIFS-376 S. Bazdenkov, T. Sato, K. Watanabe and The Complexity Simulation Group,
Multi-Scale Semi-Ideal Magnetohydrodynamics of a Tokamak Plasma; Sep. 1995

NIFS-377 J. Uramoto,
Extraction of Negative Pionlike Particles from a H2 or D2 Gas Discharge Plasma in Magnetic Field; Sep. 1995

NIFS-378 K. Akaishi,
Theoretical Consideration for the Outgassing Characteristics of an Unbaked Vacuum System; Oct. 1995

NIFS-379 H. Shimazu, S. Machida and M. Tanaka,
Macro-Particle Simulation of Collisionless Parallel Shocks; Oct. 1995

NIFS-380 N. Kondo and Y. Kondoh,
Eigenfunction Spectrum Analysis for Self-organization in Dissipative Solitons; Oct. 1995

NIFS-381 Y. Kondoh, M. Yoshizawa, A. Nakano and T. Yabe,
Self-organization of Two-dimensional Incompressible Viscous Flow in a Friction-free Box; Oct. 1995

NIFS-382 Y.N. Nejoh and H. Sanuki,
The Effects of the Beam and Ion Temperatures on Ion-Acoustic Waves in an Electron Beam-Plasma System; Oct. 1995

NIFS-383 K. Ichiguchi, O. Motojima, K. Yamazaki, N. Nakajima and M. Okamoto
Flexibility of LHD Configuration with Multi-Layer Helical Coils; Nov. 1995

NIFS-384 D. Biskamp, E. Schwarz and J.F. Drake,
Two-dimensional Electron Magnetohydrodynamic Turbulence; Nov. 1995

NIFS-385 H. Kitabata, T. Hayashi, T. Sato and Complexity Simulation Group, *Impulsive Nature in Collisional Driven Reconnection*; Nov. 1995

NIFS-386 Y. Katoh, T. Muroga, A. Kohyama, R.E. Stoller, C. Namba and O. Motojima,
Rate Theory Modeling of Defect Evolution under Cascade Damage Conditions·The Influence of Vacancy-type Cascade Remnants and Application to the Defect Production Chracterization by Microstructural Analysis; Nov. 1995

NIFS-387 K. Araki, S. Yanase and J. Mizushima,
Symmetry Breaking by Differential Rotation and Saddle-node Bifurcation of the Thermal Convection in a Spherical Shell; Dec. 1995

NIFS-388 V.D. Pustovitov,
Control of Pfirsch-Schlüter Current by External Poloidal Magnetic Field in Conventional Stellarators: Dec. 1995

NIFS-389 K. Akaishi,
On the Outgassing Rate Versus Time Characteristics in the Pump-down of an Unbaked Vacuum System; Dec. 1995

NIFS-390 K.N. Sato, S. Murakami, N. Nakajima, K. Itoh,
Possibility of Simulation Experiments for Fast Particle Physics in Large Helical Device (LHD); Dec. 1995

NIFS-391 W.X.Wang, M. Okamoto, N. Nakajima, S. Murakami and N. Ohyabu,
A Monte Carlo Simulation Model for the Steady-State Plasma in the Scrape-off Layer; Dec. 1995

NIFS-392 Shao-ping Zhu, R. Horiuchi, T. Sato and The Complexity Simulation Group,
Self-organization Process of a Magnetohydrodynamic Plasma in the Presence of Thermal Conduction; Dec. 1995

NIFS-393 M. Ozaki, T. Sato, R. Horiuchi and the Complexity Simulation Group
Electromagnetic Instability and Anomalous Resistivity in a Magnetic Neutral Sheet; Dec. 1995

NIFS-394 K. Itoh, S.-I Itoh, M. Yagi and A. Fukuyama,
Subcritical Excitation of Plasma Turbulence; Jan. 1996

NIFS-395 H. Sugama and M. Okamoto, W. Horton and M. Wakatani,
Transport Processes and Entropy Production in Toroidal Plasmas with Gyrokinetic Eletromagnetic Turbulence; Jan. 1996

NIFS-396 T. Kato, T. Fujiwara and Y. Hanaoka,
X-ray Spectral Analysis of Yohkoh BCS Data on Sep. 6 1992 Flares - Blue Shift Component and Ion Abundances -; Feb. 1996

NIFS-397 H. Kuramoto, N. Hiraki, S. Moriyama, K. Toi, K. Sato, K. Narihara, A. Ejiri,

T. Seki and JIPP T-IIU Group,
Measurement of the Poloidal Magnetic Field Profile with High Time Resolution Zeeman Polarimeter in the JIPP T-IIU Tokamak; Feb. 1996

NIFS-398 J.F. Wang, T. Amano, Y. Ogawa, N. Inoue,
Simulation of Burning Plasma Dynamics in ITER; Feb. 1996

NIFS-399 K. Itoh, S-I. Itoh, A. Fukuyama and M. Yagi,
Theory of Self-Sustained Turbulence in Confined Plasmas; Feb. 1996

NIFS-400 J. Uramoto,
A Detection Method of Negative Pionlike Particles from a H2 Gas Descharge Plasma; Feb. 1996

NIFS-401 K.Ida, J.Xu, K.N.Sato, H.Sakakita and JIPP TII-U group,
Fast Charge Exchange Spectroscopy Using a Fabry-Perot Spectrometer in the JIPP TII-U Tokamak; Feb. 1996

NIFS-402 T. Amano,
Passive Shut-Down of ITER Plasma by Be Evaporation; Feb. 1996

NIFS-403 K. Orito,
A New Variable Transformation Technique for the Nonlinear Drift Vortex; Feb. 1996

NIFS-404 T. Oike, K. Kitachi, S. Ohdachi, K. Toi, S. Sakakibara, S. Morita, T. Morisaki, H. Suzuki, S. Okamura, K. Matsuoka and CHS group;
Measurement of Magnetic Field Fluctuations near Plasma Edge with Movable Magnetic Probe Array in the CHS Heliotron/Torsatron; Mar. 1996

NIFS-405 S.K. Guharay, K. Tsumori, M. Hamabe, Y. Takeiri, O. Kaneko, T. Kuroda,
Simple Emittance Measurement of H- Beams from a Large Plasma Source; Mar. 1996

NIFS-406 M. Tanaka and D. Biskamp,
Symmetry-Breaking due to Parallel Electron Motion and Resultant Scaling in Collisionless Magnetic Reconnection; Mar. 1996

NIFS-407 K. Kitachi, T. Oike, S. Ohdachi, K. Toi, R. Akiyama, A. Ejiri, Y. Hamada, H.Kuramoto, K. Narihara, T. Seki and JIPP T-IIU Group,
Measurement of Magnetic Field Fluctuations within Last Closed Flux Surface with Movable Magnetic Probe Array in the JIPP T-IIU Tokamak; Mar. 1996

NIFS-408 K. Hirose, S. Saitô and Yoshi.H. Ichikawa
Structure of Period-2 Step-1 Accelerator Island in Area Preserving Maps; Mar. 1996